Targeting NAAA counters dopamine neuron loss and symptom progression in mouse models of parkinsonism

Francesca Palese[1,†], **Silvia Pontis**[2,†], **Natalia Realini**[2], **Alexa Torrens**[1], **Faizy Ahmed**[1], **Francesca Assogna**[3], **Clelia Pellicano**[3], **Paola Bossù**[3], **Gianfranco Spalletta**[3], **Kim Green**[4], **Daniele Piomelli**[1,5,6]

[1]Department of Anatomy and Neurobiology University of California Irvine, 92697-1275 CA, USA

[2]Drug Discovery and Development, Fondazione Istituto Italiano di Tecnologia, 16163 Genoa, Italy

[3]Laboratorio di Neuropsichiatria, IRCCS Santa Lucia Foundation, 00179 Rome, Italy

[4]Department of Neurobiology and Behavior, University of California Irvine, 92697-1275 CA, USA

[5]Department of Pharmaceutical Sciences, University of California Irvine, 92697-1275 CA, USA

[6]Department of Biological Chemistry, University of California Irvine, 92697-1275 CA, USA

Abstract

The lysosomal cysteine hydrolase *N*-acylethanolamine acid amidase (NAAA) deactivates palmitoylethanolamide (PEA), a lipid-derived PPAR-α agonist that is critically involved in the control of pain and inflammation. In this study, we asked whether NAAA-regulated PEA signaling might contribute to dopamine neuron degeneration and parkinsonism induced by the mitochondrial neurotoxins, 6-hydroxydopamine (6-OHDA) and 1-methyl-4-phenyl-1,2,3,6-tetrahydropyridine (MPTP). In vitro experiments showed that 6-OHDA and MPTP enhanced NAAA expression and lowered PEA content in human SH-SY5Y cells. A similar effect was observed in mouse midbrain dopamine neurons following intra-striatal 6-OHDA injection. Importantly, deletion of the *Naaa* gene or pharmacological inhibition of NAAA activity substantially attenuated both dopamine neuron death and parkinsonian symptoms in mice treated with 6-OHDA or MPTP. Moreover, NAAA expression was elevated in postmortem brain cortex and premortem blood-derived exosomes from persons with Parkinson's disease compared to age-matched controls. The results identify NAAA-regulated PEA signaling as a molecular control point for dopaminergic neuron survival and a potential target for neuroprotective intervention.

Introduction

The lysosomal cysteine hydrolase, *N*-acylethanolamine acid amidase (NAAA) [1,2], deactivates the lipid-derived mediator palmitoylethanolamide (PEA), an endogenous agonist of the ligand-operated transcription factor, peroxisome proliferator-activated receptor-α (PPAR-*a*)[3]. In peripheral organs, NAAA is primarily expressed in immune cells such as circulating monocytes, B-lymphocytes and tissue-resident macrophages [4], though its presence in first-order sensory neurons was also reported [Bonezzi, Khasabova]. Consistent with this cellular localization, NAAA-regulated PEA signaling at PPAR-*a* has been implicated in the control of inflammation and peripheral nociception [2,5]. In the spinal cord – where NAAA is found in neurons, microglia and oligodendrocytes [6, 7] – NAAA activity may contribute to autoimmune neuroinflammation [6,8,9] and enable the progression from acute to chronic pain after tissue injury [7].

Despite the known neuroprotective effects of PEA [10,11], thus far, investigations on the functions served by the NAAA-PEA signaling complex in the brain have been primarily focused on dopamine signaling [12] and substance use [13,14]. Interestingly, however, a large-scale study of three independent cohorts of persons with late-onset Alzheimer's disease uncovered a strong and unexpected association between elevated *Naaa* transcription and neuronal loss [15], which is suggestive of a possible pathogenic role for NAAA in neurodegeneration. Prompted by these findings, in the present study we examined whether NAAA-regulated PEA signaling might contribute to dopaminergic neuron loss induced by the mitochondrial neurotoxins, 6-hydroxydopamine (6-OHDA) and 1-methyl-4-phenyl-1,2,3,6-tetrahydropyridine (MPTP). The results show that *(i)* 6-OHDA and MPTP stimulate NAAA expression in mouse nigrostriatal dopaminergic neurons and human SH-SY5Y cells; and *(ii)* deletion of the *Naaa* gene and pharmacological inhibition of intracellular NAAA activity strongly attenuate dopamine neuron death and parkinsonian symptoms caused in mice by either of the two toxins. Finally, pointing to a possible relevance to human neurodegenerative pathologies, we found that NAAA expression is significantly elevated in postmortem brain cortex specimens and premortem blood-derived exosomes of persons with Parkinson's disease, relative to age-matched control subjects. The results identify NAAA-regulated PEA signaling as a previously unrecognized molecular checkpoint for dopaminergic neuron survival and a potential therapeutic target for neurodegeneration.

Results

Dopaminergic neurotoxins stimulate NAAA expression in human SH-SY5Y cells

We first asked whether 6-OHDA and 1-methyl-4-phenylpyridinium (MPP$^+$, the bioactive metabolite of MPTP) — two neurotoxins that cause parkinsonian symptoms in rodents and humans [16,17] — might influence NAAA expression in human SH-SY5Y cells, which express the catecholamine-producing enzyme tyrosine hydroxylase (TH) (Fig. 1B, C). Incubation with 6-OHDA (100 μM) reduced cell viability (Fig. 1A) and produced substantial increases in *Naaa* mRNA (Fig. 1D) and NAAA protein levels (Fig. 1E, F), which were accompanied by a concomitant decrease in cellular PEA content (Fig. 1G). An apparent

increase in TH fluorescence intensity was also observed ($3.6 \times 10^6 \pm 1.2 \times 10^6$??, Fig. 1B, C) but not further investigated. Of note, 6-OHDA stimulated the release into the cell culture medium of NAAA-containing CD63 and Alix positive vesicles (Fig. 1H, I). Similarly, exposing SH-SY5Y cells to MPP$^+$ (2 mM) lowered cell viability (Fig. 1J) and stimulated NAAA expression (Fig. 1K–M). A trend toward decreased PEA content was also noted, which did not reach statistical significance (Fig. 1N). The shared ability of 6-OHDA and MPP$^+$ to induce NAAA expression in SH-SY5Y cells is consistent with an involvement of this enzyme in dopaminergic neuron survival. To further evaluate this possibility, we turned to in vivo mouse models.

6-OHDA enhances NAAA expression in mouse nigrostriatal dopamine neurons

Unilateral striatal injections of 6-OHDA produced in male mice a rapid and persistent increase of NAAA immunoreactivity in dopaminergic TH-positive (TH$^+$) neurons of the ipsilateral substantia nigra (SN) pars compacta (Fig. 2A–D; separate channels: Supplementary Fig. 1, 2). Within 48 h of toxin administration, NAAA protein levels in the SN rose by approximately 30% (Fig. 2E), while the fraction of TH$^+$ cells that also expressed the enzyme rose from <1% to >15% and remained significantly elevated (≈6% of total) for the following 12 days (Fig. 2F; representative images and colocalization analysis: Supplementary Fig. 3). Unbiased proteomic profiling of nigral tissue at the 48-h time-point revealed that heightened NAAA expression was part of a broad reaction to the toxin that involved changes in 417 quantifiable proteins (from a total of 1164 detected; Supplementary Table 1 and Supplementary Fig. 4), most of which (378/417) were underrepresented in damaged SN (Supplementary Table 2). Consistent with the mechanism of action of 6-OHDA, which is known to impair mitochondrial complex I function [18,19] analysis of downregulated proteins revealed enrichment in components of oxidative phosphorylation (particularly complex I) as well as pathways of fatty-acid and glycan metabolism (Supplementary Fig. 5). Parallel lipid analyses showed that the early surge in NAAA expression was accompanied by a ≈30% decrease in nigral PEA content (Fig. 2G), whereas levels of the less-preferred NAAA substrate, oleoylethanolamide (OEA) [20,21], were only marginally affected (Fig. 2H).

Two weeks after 6-OHDA injection, when inflammation had spread to the dorsolateral striatum – as evidenced by enhanced transcription of inflammatory cytokines (Fig. 3A) and damage to striatal TH$^+$ fibers (Supplementary Fig. 6) – NAAA levels rose sharply in cells expressing the microglia/macrophage marker, ionized calcium-binding adaptor molecule 1-positive (Iba-1$^+$) (Fig. 3 B–D). NAAA$^+$ microglia were primarily found in proximity of damaged nigral TH$^+$ neurons (Fig. 2C, D; separate channels: Supplementary Fig. 2) and striatal TH$^+$ fibers (Fig. 3E, F; separate channels: Supplementary Fig. 6). The results are consistent with those reported above for SH-SY5Y cells (Fig. 1C–F) and indicate that enhanced NAAA expression in midbrain dopamine neurons may be an early component of the toxic response to 6-OHDA in mice. As neuroinflammation develops, NAAA induction may extend to reactive microglia mobilized to damaged neural structures.

Genetic and pharmacological NAAA ablation attenuate 6-OHDA-induced neurotoxicity

To investigate NAAA's possible roles in 6-OHDA-induced neurotoxicity, we used genetically modified mice that express the protein in a frame-shifted catalytically inactive form ($Naaa^{-/-}$ mice). The mutants constitutively lack $Naaa$ mRNA as well as NAAA protein and activity (Supplementary Fig. 7), and do not compensate for this absence with altered transcription of isofunctional enzymes (fatty acid amide hydrolase) [22], PEA-producing enzymes (N-acyl-phosphatidylethanolamine phospholipase D) [23] or other lysosomal lipid hydrolases (acid ceramidase and β-glucocerebrosidase) [22,23] (Supplementary Fig. 7). As shown in Figure 4, homozygous NAAA deletion protected male mice from the cellular, neurochemical, and behavioral consequences of 6-OHDA injection. Three weeks after toxin administration, comparison with wild-type littermates showed that $Naaa^{-/-}$ mice had (*i*) improved survival of nigral TH$^+$ neurons (Fig. 4A); (*ii*) higher striatal levels of dopamine (Fig. 4B) and dopamine metabolites (Supplementary Fig. 8); and (*iii*) greater density of striatal TH$^+$ fibers (Fig. 4C). Moreover, $Naaa^{-/-}$ mice displayed (*iv*) prolonged latency to fall in the rotarod performance test (Fig. 4D); (*v*) attenuated motor responses (contralateral rotations) to the dopaminergic agonist apomorphine (0.1 mg/kg, subcutaneous; Fig. 4E); and (*vi*) lower mortality rate (Fig. 4F). Importantly, heterozygous $Naaa^{+/-}$ mice were also resistant to 6-OHDA, but less so than their homozygous littermates (Fig. 4A–F). The gene-dose-dependent neuroprotection caused by NAAA deletion points to a role for this enzyme in the control of dopamine neuron survival.

Supporting this conclusion, we found that subchronic treatment with the systemically active NAAA inhibitor ARN19702 [8] phenocopied genetic NAAA deletion. In male wild-type mice exposed to 6-OHDA, a 3-week twice-daily regimen with ARN19702 (30 mg/kg, intraperitoneal, starting on the day of 6-OHDA administration) exerted a set of neuroprotective effects that included, in the SN, enhanced survival of TH$^+$ neurons (Fig. 4G) and, in the dorsolateral striatum, increased dopamine and dopamine metabolite content (Fig. 4H, Supplementary Fig. 9) and density of TH$^+$ fibers (Fig. 4I). Additionally, the NAAA inhibitor prolonged the latency to fall in the rotarod test (Fig. 4J), attenuated motor responses to apomorphine (Fig. 4K) and decreased animal mortality (Fig. 4L). Thus, as seen with $Naaa$ deletion, pharmacological inhibition of NAAA activity enhances dopamine neuron survival and improves the behavioral repertoire of mice treated with 6-OHDA.

Genetic or pharmacological NAAA ablation attenuates MPTP-induced neurotoxicity

Next, we asked whether the neuroprotective effects of NAAA removal generalize to MPTP-induced neurotoxicity [24]. Within 7 days of administration, MPTP produced in female wild-type mice a substantial loss of SN dopamine neurons (Fig. 5A and Supplementary Figure 10) and a decrease in striatal dopamine and dopamine metabolite levels (Fig. 5B and Supplementary Fig. 11) and TH$^+$ fiber density (Fig. 5C and Supplementary Fig.12). These morphological and neurochemical events were accompanied by a worsened performance in the rotarod test (Fig. 5D) and by marked animal mortality (Fig. 5E). Importantly, the effects of MPTP were substantially attenuated in $Naaa^{-/-}$ mice (Fig. 5A–E). As seen in the 6-OHDA model, treatment with ARN19702 (30 mg/kg, twice daily, intraperitoneal, starting the day before MPTP administration) phenocopied $Naaa$ deletion, improving dopamine neuron survival (Fig. 5F and Supplementary Fig. 10), increasing striatal dopamine content

(Fig. 5G) and fiber number (Fig. 5H and Supplementary Fig. 12), normalizing behavior in the rotarod test (Fig. 5I) and curbing animal mortality (Fig. 5J). Collectively, the results suggest that NAAA-regulated PEA signaling protects nigral dopamine neurons against 6-OHDA- and MPTP-induced toxicity. Both male and female mice appear to be protected.

Mechanistic insights

To gain insights into possible mechanisms through which NAAA might influence neuronal survival, we compared the nigral proteomes of $Naaa^{-/-}$ and wild-type mice 48 h after 6-OHDA administration, when NAAA expression is maximal in dopamine neurons but still undetectable in microglia. Analyses of lesioned SN tissue identified 607 differentially expressed proteins, most of which (603) were overrepresented in $Naaa^{-/-}$ mice compared to wild-type controls (Supplementary Table 7). Interrogation of the data using the Database for Annotation, Visualization, and Integrated Discovery (DAVID) [25] showed that proteins upregulated in $Naaa^{-/-}$ mice included many components of oxidative phosphorylation (Fig. 6A), carbon metabolism (Fig. 6C) and lipid and glycan metabolism (Fig. 6D). Similarly, Gene Ontology (GO) analysis revealed a substantial enrichment in proteins that are (*i*) part of the Krebs' cycle, oxidative phosphorylation, and glycolysis (GO category 'biological process'); (*ii*) involved in ATP synthesis, proton transport and redox function ('molecular function); and (*iii*) localized to the mitochondrial inner membrane and cytoskeleton ('cellular component') (Supplementary Fig. 14). In contrast with the profound changes observed in lesioned SN, parallel studies of intact SN found only minor differences between $Naaa^{-/-}$ and wild-type mice (Fig. 6B, E, F).

The marked impact of NAAA deletion on cellular bioenergetic pathways led us to hypothesize that members of the PGC-1 family, which are crucial upstream regulators of those pathways and have been implicated in dopamine neuron survival [26,27,28,29], might be involved in the neuroprotective effects of NAAA ablation. Supporting this conclusion, a closer inspection of the proteomics data identified type-β peroxisome proliferator-activated receptor-γ coactivator-1 (PGC-1β) as one of the proteins deregulated by 6-OHDA (Fig. 8A, Supplementary Table 7: *replicate 2, line 641*). Western blot analyses confirmed that PGC-1β is overrepresented in lesioned SN of $Naaa^{-/-}$ mice, relative to lesioned SN of wild-type controls (Fig. 7 B, C), and further showed that another key member of the PGC-1 family, PGC-1α, is also subject to NAAA regulation (Fig. 7 D, E). It is noteworthy that PGC-1α and β were both underrepresented in lesioned SN of wild-type mice – as seen in persons with Parkinson's disease [27] – whereas, in $Naaa^{-/-}$ mutants, they were constitutively elevated and did not change in response to 6-OHDA (Fig. 7 B–E).

NAAA expression is abnormally elevated in persons with Parkinson's disease

Since mitochondrial dysfunction and respiratory chain impairment are established pathological features of sporadic Parkinson's disease [30,31], we explored the possible implication of NAAA in this neurodegenerative disorder. *Naaa* mRNA and NAAA protein levels were significantly elevated in postmortem specimens of brain cortex from persons with Parkinson's disease (n=43) relative to age-matched controls (n=46) (Fig. 8A, B; demographic and clinical data are reported in Supplementary Table 15). Because postmortem conditions influence the quality of results obtained with human brain tissue

[32], we also measured NAAA protein levels in blood-derived extracellular vesicles from a separate small cohort of patients with Parkinson's disease (n=11; average age at collection: 54.7 ± 14.8 years, disease stage I-II; mean ± SD) and age-matched control subjects (n=12; average age: 49.2 ± 10.7 years) (demographic and clinical data are shown in Supplementary Table 16). In this pilot study too, we observed a marked NAAA elevation in persons with Parkinson's disease compared to controls (Fig. 8C, D). Immunohistochemical analyses of brain cortex from a female Parkinson's patient showed a primary localization of immunoreactive NAAA in neurons and microglia (Fig. 8E and F; separate channels: Supplementary Fig. 15). As previously reported for mouse spinal cord [6], NAAA immunoreactivity was undetectable in astrocytes (Fig. 8G; separate channels: Supplementary Fig. 15) even though these cells are thought to contain relatively high levels of *Naaa* mRNA (http://neuroexpresso.org).

Discussion

NAAA catalyzes the hydrolytic deactivation of the lipid-derived PPAR-α agonist, PEA, an important regulator of nociception and inflammation [1,2]. The objective of the present study was to determine whether this enzyme might also contribute to the neurodegenerative effects of 6-OHDA and MPTP, two neurotoxins that cause parkinsonian symptoms by disrupting the mitochondrial respiratory chain in nigrostriatal dopaminergic neurons [16,17]. We carried out three experiments to test this idea. First, we investigated the effects of 6-OHDA and MPTP on NAAA expression. Incubation of human SH-SY5Y cells in cultures with either toxin produced a substantial increase in *Naaa* mRNA and NAAA protein. Similar changes were observed in mouse midbrain, where intrastriatal injections of 6-OHDA stimulated NAAA expression, first in nigrostriatal dopamine neurons and subsequently in microglia recruited to the sites of injury. These observations motivated a second set of experiments, in which we examined whether removal of the *Naaa* gene or inhibition of NAAA activity might attenuate dopamine neuron death caused in mice by administration of 6-OHDA or MPTP. We found that both genetic and pharmacological NAAA ablation increased dopamine neuron viability and countered the motor dysfunction elicited by the toxins. Finally, we measured NAAA mRNA and protein levels in premortem blood-derived vesicles and postmortem brain cortex specimens of persons with Parkinson's disease. The analyses uncovered evidence for elevated NAAA expression in these subjects, compared to age- and sex-matched controls. Collectively, the results identify NAAA as a molecular control point for the survival of nigrostriatal dopamine neurons and a potential therapeutic target for neurodegenerative pathologies such as Parkinson's disease.

It is plausible that NAAA-regulated PEA signaling influences dopamine neuron viability by modulating neuroinflammation [6,8,9]. Our findings point, however, to a more complex scenario. In mice treated with 6-OHDA, the rise in NAAA expression is initially confined to dopamine neurons (Fig. 2) and only later extends to reactive microglia (Fig. 3). The 'neuronal' phase of NAAA induction begins within 24 h of exposure to the toxin (Fig. 2 and Supplementary Fig. 3) – that is, well before the appearance of overt signs of neuroinflammation – and is part of a broad program that includes the suppression of protein networks responsible for mitochondrial biogenesis and cellular respiration (Supplementary Fig. 4 and 5). This suggests that PEA-mediated signaling at PPAR-α may protect dopamine

neurons, at least in part, by preserving their bioenergetic potential – as recently proposed for spinal cord neurons after peripheral organ injury [7] – and that pathological NAAA induction might undermine this protection. Supporting this view, our results also indicate that NAAA deletion *(i)* prevents the disruptive effects of 6-OHDA on cellular bioenergetic pathways (Fig. 6); and *(ii)* normalizes expression of the transcription coactivators, PGC-1α and PGC-1β, which are suppressed after 6-OHDA challenge (Fig. 7 C). PGC-1α and PGC-1β serve pivotal functions in metabolic control and, importantly, have been implicated in dopamine neuron survival [26] and the pathogenesis of Parkinson's disease [27,33]. Similar roles have been ascribed to PPAR-α [34,35], PEA's primary receptor and obligatory PGC-1α partner.

The possible relevance of our results to sporadic Parkinson's disease in humans requires consideration. First, the animal studies presented here relied on two toxin models which, though well-characterized and widely used, do not recapitulate the slow progressive nature of sporadic Parkinson's disease [36]. A possible alternative, which will be evaluated in future work, is offered by the α-synuclein pre-formed fibril model, which is gaining traction after its recent standardization [37]. Second, due to limited availability, our human studies included a relatively small number of premortem subjects and postmortem samples, and focused on cortex rather than basal ganglia. Additional work is clearly needed. However, despite these limitations, our results do suggest that NAAA expression may be elevated in postmortem brain cortex from persons with advanced Parkinson's disease (average age of death: 76.5 ± 4.9 years; disease duration: 15.3 ± 8.3 years) as well as in blood-derived vesicles from persons at stages I and II of the disease, according to Hoehn and Yahr (average age at collection: 54.7 ± 14.8 years; disease duration: 3.58 ± 2.6 years). This finding raises two critical questions, namely, what genetic or environmental stimuli might be responsible for triggering NAAA elevation? And, when could such elevation occur in an individual's lifespan and in which organ system(s)? The heterogeneous etiology, long prodromic phase, and slow progression of Parkinson's disease [38] make answering these questions especially arduous. One possible scenario, however, is that risk factors for Parkinson's disease (e.g. exposure to pollutants, etc.) [38], may directly or indirectly enhance NAAA expression, as suggested by the enzyme's inducible nature [7]. Alternatively, or possibly complementarily, NAAA upregulation may result from neuronal damage caused by accumulation of insoluble α-synuclein aggregates, a neuropathological hallmark of Parkinson's disease [39]. Given the multisystem spread of Parkinson's disease pathology [40], both events might take place in brain, peripheral organs, or both.

In conclusion, the present report provides multiple lines of evidence suggesting that NAAA may contribute to the control of nigrostriatal dopamine neuron survival and might thus offer a druggable target for therapeutic intervention in neurodegenerative pathologies.

Materials and methods

Ethics statement

Investigations were conducted in accordance with the Declaration of Helsinki as well as with relevant international guidelines. They were approved by each of the authors' institutional review boards. Human studies were approved by the Ethical Committee of I.R.C.C.S. Santa

Lucia Foundation (CE-AG4-Prog.149). All the participants or related caretakers gave their written consent to the enrollment.

Chemicals

6-OHDA hydrochloride, MPP⁺ iodide, chloral hydrate, ketamine, xylazine, paraformaldehyde, MPTP, dopamine, serotonin, homovanillic acid (HVA), 3,4-dihydroxyphenylacetic acid (DOPAC), ascorbic acid, and [$^2H_5$]-benzoyl chloride were purchased from Sigma Aldrich (Saint Louis, MO). [$^2H_4$]-PEA and [$^2H_4$]-OEA were from Cayman Chemical (Ann Arbor, MI, USA). Tandem Mass Tag™ 6-plex (TMTsixplex™) reagents kits for isotopic labeling were from Thermo Fisher Scientific (Waltham, MA, USA). All analytical solvents were of the highest grade, and were obtained from Honeywell (Muskegon, MI) or Sigma-Aldrich. ARN19702 was synthetized as described [8].

Cell cultures

SH-SY5Y cells were purchased from Sigma Aldrich and cultured at 37°C and 5% CO_2 in Dulbecco's Modified Eagle's Medium (DMEM) (Euroclone, Milan, Italy) supplemented with 10% fetal bovine serum (FBS, Thermo Fisher Scientific), L-glutamine (2 mM) and antibiotics (Euroclone). Cells were incubated with 6-OHDA (100 μM), MPP⁺ (2 mM) or their respective vehicles (6-OHDA: saline containing 0.2% ascorbic acid; MPP⁺: complete DMEM) for the indicated times.

Postmortem human brain specimens

Postmortem brain cortex samples were obtained from the Banner Sun Health Research Institute [41, 42] Specimens from 46 control subjects and 43 patients with postmortem interval 1.25 – 4.83 h were used to prepare mRNA and protein extracts and to conduct morphological analyses, as described below. Detailed demographic and clinical information are provided in Supplementary Table 15.

Human study subjects

Potential study participants were assessed at the Laboratory of Neuropsychiatry of the I.R.C.C.S. Santa Lucia Foundation in Rome. Inclusion criteria for Parkinson's disease patients were: (i) diagnosis of idiopathic Parkinson's disease according to the international guidelines [43] (ii) Mini-Mental State Examination (MMSE) score 26 and no dementia according to the Movement Disorder Society (MDS) clinical diagnostic criteria [44]. Exclusion criteria were (i) presence of major non stabilized medical illnesses; (ii) known or suspected history of alcoholism, psychoactive drug dependence, head trauma, and mental disorders (apart from mood or anxiety disorders) according to the DSM-IV criteria [45]; (iii) history of neurological diseases other than idiopathic Parkinson's disease; (iv) unclear history of chronic dopaminergic treatment responsiveness; and (v) MRI scans lacking signs of focal lesions as computed according to a semi-automated method [46]. All patients included in the study were under stable dopaminergic therapy and were at stage I or II of the disease. Furthermore, they were not receiving Deep Brain Stimulation and were not under continuous dopaminergic stimulation by subcutaneous apomorphine or intrajejunal L-DOPA. Inclusion criteria for control subjects were: (i) vision and hearing sufficient

for compliance with testing procedures; (ii) laboratory values within the appropriate normal reference intervals; and (iii) neuropsychological domain scores above the cutoff scores, corrected for age and educational level, identifying normal cognitive level in the Italian population. Exclusion criteria were: (i) dementia diagnosis, according with DSM-V criteria or MCI according with Petersen criteria and confirmed by a comprehensive neuropsychological battery; and (ii) MMSE score < 26 according with standardized norms for the Italian population [47]. Sociodemographic and clinical characteristics of study participants are reported in Supplementary Table 16. Blood samples (10 mL) were collected after overnight fasting (11 ± 1 h).

Animals

All procedures were performed in accordance with the Ethical Guidelines of the European Union (directive 2010/63/EU of 22 September 2010), National Institutes of Health guidelines and the Italian Ministry of Health and were approved by the Institutional Animal Care and Use Committee of the University of California, Irvine. C57BL/6 mice (20–35 g) were purchased from Charles River (Wilmington, MA, USA). Male mice were used for 6-OHDA experiments, female mice were used for MPTP studies. B6N-Atm1BrdNaaatm1a(KOMP)wtsi/WtsiH mice ($Naaa^{-/-}$) were generated at the Welcome Trust Sanger Institute and obtained from Jackson Labs (Bar Harbor, ME, USA) [6]. All mice were group-housed in ventilated cages and had free access to food and water. They were maintained under a 12h light/dark cycle (lights on at 8:00 am) at controlled temperature (21 ± 1°C) and relative humidity (55% ± 10%). All efforts were made to minimize animal suffering and to use the minimal number of animals required to produce reliable results.

6-OHDA and MPTP-induced neurotoxicity

6-OHDA administration was performed as previously described [48] (for further details see Supplementary). MPTP was dissolved at the concentration of 18 mg/kg in ice cold saline and administered by i.p. injection every 2h for a total of 4 doses over an 8-h period in a single day, as previously described [24].

Drug treatments

ARN19702 was dissolved in a vehicle composed of sterile saline containing PEG-400 (15%, vol/vol) and Tween (15%). The drug (30 mg/kg, i.p.) or its vehicle was injected twice a day at approximately 8:00 a.m. and 6:00 p.m. Treatment started either on the day of 6-OHDA injection and was continued for the following 3 weeks, or the day before MPTP administration and lasted 7 days.

Mouse tissue processing and immunohistochemistry

Mice were anaesthetized and perfused transcardially with ice-cold saline, followed by ice-cold paraformaldehyde (PFA, 4%). The brains were excised and stored in sucrose (25% in PBS) at 4°C. Three series of sections (thickness 40 μm) were collected in the coronal plane using a cryostat and stored at −20°C. Double and triple immunostaining protocols were performed by sequential incubation with primary antibodies (1:200; Abcam, Cambridge, UK, Supplementary Table 14) followed by secondary Alexa Fluor 488 antibodies (1:1000;

Invitrogen). Images were collected using a Nikon A1 confocal microscope with a $60 \times$ 1.4 numerical aperture objective lens. The assessment of colocalization was performed using the NIH ImageJ Just Another Colocalization plug-in (JACoP) (available at http://rsb.info.nih.gov/ij/plugins/track/jacop.html).

Human tissue processing and immunohistochemistry

Postmortem human cortex samples were sectioned (thickness 40 μm) using a cryostat and stored at −20°C. Slices were fixed in ice-cold PFA (4% in PBS) and double immunostaining protocols were performed by sequential incubation with previously validated [7] primary antibodies (Supplementary Table 14) followed by secondary Alexa Fluor antibodies (1:1000; Invitrogen). Images were collected using an Olympus (Tokyo, Japan) FV3000 confocal microscope with a 40×1.25 numerical aperture objective lens.

Stereological measurements

Dopamine neurons of the SN count was performed as described [48]. Briefly, unbiased sampling and blinded stereological counting were performed using the optical fractionator probe of the Stereo Investigator software (MBF Bioscience, Williston, VT, USA). Parameters used included a 60x oil objective, a counting frame size of 60×60, a sampling site of 100×100, a dissector height of 15 μm, 2 μm guard zones. The Gunder's coefficient of error was less than 0.1. A total of 5 animals per group were used and 5 to 8 sections per animal were counted in the red/green channel.

Cell viability

The CellTiter-Glo® luminescent cell viability assay (Promega, Milan, Italy) was used to determine the number of viable cells in the culture.

Exosome isolation

One mL of human plasma was incubated with 0.5 mL of Invitrogen total exosome isolation reagent (Thermo Fisher Scientific) overnight at 4°C, then centrifuged at 10,000 x g for 1h at 4°C. Pellets were resuspended in 2 volumes of radioimmunoprecipitation assay buffer (RIPA, 150 μL, 50 mM Tris-HCI pH 7.4, 1% NP40, 0.5% Na-deoxycholate, 0.1% SDS, 150 mM NaCI, 2mM EDTA), homogenized and sonicated. Thirty μg of protein was used for western blot analyses. Cell media from 6-OHDA- or vehicle-treated SH-SY5Y cells were collected after 8 h of incubation and centrifuged at 800 x g for 10 min at 4°C. Supernatants were filtered using a 0.22 μm filter and centrifuged at 100,000 x g for 90 min at 4°C. Pellets were resuspended in 0.5 mL PBS containing a proteinase inhibitor cocktail (Thermo Fisher Scientific) and centrifuged again at 100,000 x g for 90 min at 4°C. Supernatants were collected and 30 μg of protein were used for western blot analyses to verify exosome markers (CD63 and Alix).

Western blot analyses

Human or mouse tissues were homogenized in RIPA buffer (150 μL). PGC1-α was identified and quantified in nuclear-enriched fractions. Briefly, brain tissue dissected from control and lesioned hemispheres was homogenized in buffer [v/w=5:1; 10 mM Hepes-

KOH (pH 7.4), 0.25 M sucrose, proteinase inhibitor cocktail (Sigma)]. Homogenates were centrifuged at 900 x g for 10 min. Pellets were collected, homogenized again, and centrifuged at 900 x g for 10 min, to yield the nuclear fraction (pellet). Proteins were denatured in sodium dodecyl sulfate (SDS, 8%) and β-mercaptoethanol (5%) at 95°C for 5 min. After separation by SDS-PAGE on a 4–15% gel under denaturing conditions, the proteins were electrotransferred to nitrocellulose membranes. The membranes were blocked and incubated overnight with primary antibodies in I-block solution (Thermo Fisher Scientific), followed by incubation with the corresponding secondary antibody (Invitrogen) in tris-buffered saline at room temperature for 1h. Band detection was performed with FLA-9000 Starion (Fujifilm Life Science, USA), or Fluorchem R (ProteinSimple, San Jose, CA, USA). Antibody sources and dilutions are shown in Supplementary Table 14.

Lipid extraction and liquid chromatography-mass spectrometry (LC/MS) analysis

Cell and tissue levels of PEA and OEA were measured as described [49] (for further details see Supplementary).

NAAA activity assay

NAAA activity measurement was conducted on lysosomal-enriched samples as previously described [50] (for further details see Supplementary).

Real-Time quantitative PCR

Total RNA was prepared from tissue samples or cell pellets using the Ambion PureLink RNA minikit (Life Technologies, Carlsbad, CA, USA) as directed by the supplier. Samples were treated with DNase (PureLink DNase, Life Technologies) and cDNA synthesis was carried out using the Super-Script VILO cDNA synthesis kit (Life Technologies) according to the manufacturer's protocol using purified RNA (1 μg). The amplification of cell extracts cDNA was conducted using the iQ SYBR Green SuperMix (Life Technologies) according to the manufacturer's instructions. Primers were purchased from Origene Technologies (Rockville, MD, USA) with the following sequence: forward sequence: ATTACGACCACTGGAAGCCAGC; reverse sequence: GGAAAAGTGCCTCCAGGCTGAG. Quantitative PCR was performed using a ViiA7 instrument (ViiATM 7 real-time PCR system, Life Technologies). Ct values were calculated as previously reported [48]. Quantification of tissue extracts was performed using the TaqMan 5′ nuclease activity from the TaqMan Universal PCR Master Mix, fluorogenic probes, and oligonucleotide primers.

Proteomic analyses

Sample preparation: Midbrain tissue fragments containing the left or right SN were dissected from 3 independent biological replicates and homogenized in RIPA buffer. Protein concentrations were measured using the BCA assay, and equal amounts of protein were used. Samples were isotopically labeled using TMT sixplex kits [51], according to the manufacturer's instruction. Samples were reduced with dithiothreitol, alkylated with iodoacetic acid and labeled using TMT tags. After pooling the six conditions, the total protein content from each replicate (150 μg) was separated on precast polyacrylamide gels

(Thermo Fisher Scientific). Each lane was cut into 12 slices and in-gel protein digestion was performed[52]. The samples were recovered, dried under N_2, and dissolved in 50 μL of water containing acetonitrile (3%) and formic acid (0.1%) for LC-MS/MS analysis.

LC-MS/MS analyses: Tryptic peptide mixtures were analyzed using a Synapt G2 QToF equipped with a nanoACQUITY liquid chromatographer and a nanoSpray ion source. Peptides were separated on a BEH nanobore column (75 μm ID x 25 cm length) using a linear gradient of acetonitrile in water from 3% to 55% in 3 h, followed by a washout step with 90% acetonitrile (10 min) and a reconditioning step in 3% acetonitrile for 20 min. Flow rate was set to 300 nL/min. Spray voltage was 1.6kV, cone voltage was 28V, spray gas was 0.3 L/min. Survey spectra were acquired over the $m/z = 50–1600$ scan range. Multiply charged ions (2+,3+ and 4+) between $m/z = 300$ and 1400 were selected as precursors for DDA tandem mass analysis and fragmented in the trap region of the instrument. Collision energy values were automatically selected by the software using dedicated charge-state dependent CE/m/z profiles. Every 60s, a single leu-enkefalin (2 ng/mL) MS scan was acquired by the LockMass ion source for spectra recalibration.

Data analysis: Acquired raw data files were processed using PLGS software to recalibrate the mass spectra and generate the precursor-fragments peak list. Protein identification and quantification was performed by interrogating the SwissProt database using MASCOT Server software. The search parameters were set as follows, quantification: TMT6plex; fixed modifications: carbamidomethyl (C), TMT6plex (N-term), TMT6plex (K); variable modifications: acetyl (K), acetyl (N-term), deamidated (NQ), methyl (DE), oxidation (M), phospho (ST), phospho (Y); peptide tolerance: 30ppm; fragment tolerance: 0.5Da; maximum allowed missed cleavages: two. At least two peptides were required for a positive protein identification and quantification. A significance threshold of P>0.05 was set for protein identification in the MASCOT search. All the proteins identified and quantified from all the biological replicates were retained. Proteins sharing the same set or subset of peptides were considered as a single entry (MASCOT Protein Families). Two different data analyses were then performed on the same data set. We first investigated the alterations caused by 6OHDA on the brain of naïve animals. For this purpose, only the ratio between 129 and 130 reporter ions was calculated and reported. Protein expression ratio was normalized by the average ratio of all the peptides assigned to proteins. A standard deviation of the protein expression ratios was calculated for all the proteins quantified in at least two out of three replicates. All the corresponding data are available in Supplementary Table 1. We then evaluated the role of the genotype ($NAAA^{-/-}$ versus WT) on the expression profiles of proteins in the three biological conditions: naïve animal, lesioned and contralateral side of the brain. For this purpose, three ratios were measured using the 6plex TMT reporter ions and the reporting function of MASCOT: 126/129 for the lesion side, 127/130 for the contralateral side and 128/131 for the naïve brain. Protein expression ratio was normalized by the average ratio of all the peptides assigned to proteins. Protein expression ratio was normalized by the average ratio of all the peptides assigned to proteins. A standard deviation of the protein expression ratios was calculated for all the proteins quantified in at least 2 out of three replicates. All the corresponding data are available in Supplementary Table 2.

Neurotransmitter measurements

6-OHDA experiments: Dopamine and metabolites in 6-OHDA treated mice were measured as previously reported [48] (for further details see Supplementary).

MPTP experiments: The dorsal striatum (~15 mg) was homogenized in 0.5 mL ice-cold acetonitrile containing 1% formic acid and 10 μg/mL internal standard ($[^2H_5]$-benzoyl-HVA, $[^2H_5]$-benzoyl -DOPAC, $[^2H_5]$-benzoyl- DA, $[^2H_5]$-benzoyl-serotonin). After stirring and centrifugation, the supernatants were transferred to 5 mL glass vials. Tissue pellets were rinsed with water/acetonitrile (1:4, v/v; 0.2 mL), stirred, centrifuged and supernatants were pooled with the first eluate. Eluates were dried under N_2 and reconstituted in 0.1 mL of 100 mM Na_2BO_4 and vortexed. Benzoyl Chloride (5 μL) was added and the mixture was allowed to incubate at room temperature for 30 min. After incubation, methanol (50 μL) was added to quench the reaction, followed by acetonitrile to dissolve the resulting precipitate. Samples were filtered through Agilent Captiva syringe filters in to deactivated glass inserts (0.2 mL) placed inside amber glass vials (2 mL; Agilent Technologies). LC separations were carried out using a 1200 series LC system (Agilent Technologies), consisting of a binary pump, degasser, thermostated autosampler and column compartment coupled to a 6410B triple quadrupole mass spectrometric detector (MSD; Agilent Technologies). Analytes were separated on an Eclipse PAH C18 column (1.8 μm, 2.1×50.0 mm; Agilent Technologies). The flow rate was 0.4 mL/min, using the following gradient conditions: 0–7.0 min 40% B (methanol containing 0.1% formic acid and 5 mM ammonium formate) in solvent A (water containing 0.1% formic acid and 5 mM ammonium formate) to 62% B, 7.01–8.0 95% B, 8.01–10.0 min 40% B for re-equilibration. The column temperature was maintained at 30°C and the autosampler at 9°C. The total analysis time, including re-equilibrium, was 10 min. The injection volume was 2 μL. The MS was operated in the positive electrospray ionization (ESI) mode, and analytes were quantified by multiple reaction monitoring (MRM) of the following transitions: benzoyl-DA 466.2 > 77.1 *m/z*, $[^2H_5]$-benzoyl-DA 481.3 > 110.1 *m/z*, benzoyl-DOPAC 394.1 > 77.1 m/z, $[^2H_5]$-benzoyl-DOPAC 404.2 > 110.1 *m/z*, benzoyl-SE 385.2 > 77.1 *m/z*, $[^2H_5]$-benzoyl-SE 395.2 > 110.1 m/z, benzoyl-HVA 304.1 > 77.1 *m/z*, $[^2H_5]$-benzoyl-HVA 309.2 > 110.1 *m/z*. The capillary voltage was set at 2500 V. The source temperature was 350°C and gas flow was set at 10.0 L/min. Nebulizer pressure was set at 45 psi. Collision energy and fragmentation voltage were set for each analyte as reported. The MassHunter software (Agilent Technologies) was used for instrument control, data acquisition, and data analysis.

Apomorphine-induced rotations

Apomorphine-induced rotations were quantified as previously reported [48] (fort further details see Supplementary).

Rotarod test

Behavioral testing on a mouse rotarod apparatus equipped with a 3 cm diameter rod (Ugo Basile, Varese, Italy) was performed on day 21 after surgery, or 7 days post MPTP intoxication, with an accelerating rod (from 15 to 25 rpm in 150 s). All mice were pre-trained one week before the treatments. The training consisted of 5 consecutive runs at

20 rpm or until the mice were able to maintain themselves for 300 s on the rotating rod. Subsequently, a new test series with accelerating conditions was started. One day prior to surgery, baseline values were obtained under the same conditions.

Statistical analyses

Data were analyzed as described in figure legends using GraphPad Prism version 5 for Windows (La Jolla, California, USA). For data with Gaussian distribution, parametric statistical analysis was performed using the two-tailed Student's t-test for two groups; one-way or two-way analysis of variance (ANOVA) was applied for multiple comparisons with Bonferroni post hoc analysis for data meeting homogeneity of variance.

Supplementary Material

Refer to Web version on PubMed Central for supplementary material.

Acknowledgements

Data availability

This study includes no data deposited in external repositories.

References

[1]. Ueda N, Tsuboi K, Uyama T, N-acylethanolamine metabolism with special reference to N-acylethanolamine-hydrolyzing acid amidase (NAAA), Prog. Lipid Res (2010). doi:10.1016/j.plipres.2010.02.003.

[2]. Piomelli D, Scalvini L, Fotio Y, Lodola A, Spadoni G, Tarzia G, Mor M, N -Acylethanolamine Acid Amidase (NAAA): Structure, Function, and Inhibition, J. Med. Chem (2020). doi:10.1021/acs.jmedchem.0c00191.

[3]. Pontis S, Ribeiro A, Sasso O, Piomelli D, Macrophage-derived lipid agonists of PPAR-α as intrinsic controllers of inflammation, Crit. Rev. Biochem. Mol. Biol (2016). doi:10.3109/10409238.2015.1092944.

[4]. Ribeiro A, Pontis S, Mengatto L, Armirotti A, Chiurchiù V, Capurro V, Fiasella A, Nuzzi A, Romeo E, Moreno-Sanz G, Maccarrone M, Reggiani A, Tarzia G, Mor M, Bertozzi F, Bandiera T, Piomelli D, A Potent Systemically Active N-Acylethanolamine Acid Amidase Inhibitor that Suppresses Inflammation and Human Macrophage Activation, ACS Chem. Biol (2015). doi:10.1021/acschembio.5b00114.

[5]. Piomelli D, Sasso O, Peripheral gating of pain signals by endogenous lipid mediators, Nat. Neurosci (2014). doi:10.1038/nn.3612.

[6]. Pontis S, Palese F, Summa M, Realini N, Lanfranco M, De Mei C, Piomelli D, N-Acylethanolamine Acid Amidase contributes to disease progression in a mouse model of multiple sclerosis, Pharmacol. Res (2020). doi:10.1016/j.phrs.2020.105064.

[7]. Fotio Y, Jung KM, Palese F, Obenaus A, Tagne AM, Lin L, Rashid TI, Pacheco R, Jullienne A, Ramirez J, Mor M, Spadoni G, Jang C, Hohmann AG, Piomelli D, NAAA-regulated lipid signaling governs the transition from acute to chronic pain, Sci. Adv (2021). doi:10.1126/sciadv.abi8834.

[8]. Migliore M, Pontis S, Fuentes de Arriba AL, Realini N, Torrente E, Armirotti A, Romeo E, Di Martino S, Russo D, Pizzirani D, Summa M, Lanfranco M, Ottonello G, Busquet P, Jung KM, Garcia-Guzman M, Heim R, Scarpelli R, Piomelli D, Second-Generation Non-Covalent NAAA Inhibitors are Protective in a Model of Multiple Sclerosis, Angew. Chemie - Int. Ed (2016). doi:10.1002/anie.201603746.

[9]. Sgroi S, Romeo E, Di Fruscia P, Porceddu PF, Russo D, Realini N, Albanesi E, Bandiera T, Bertozzi F, Reggiani A, Inhibition of N-acylethanolamine-hydrolyzing acid amidase reduces T cell infiltration in a mouse model of multiple sclerosis, Pharmacol. Res (2021). doi:10.1016/j.phrs.2021.105816.

[10]. Skaper SD, Facci L, Barbierato M, Zusso M, Bruschetta G, Impellizzeri D, Cuzzocrea S, Giusti P, N-Palmitoylethanolamine and Neuroinflammation: a Novel Therapeutic Strategy of Resolution, Mol. Neurobiol (2015). doi:10.1007/s12035-015-9253-8.

[11]. Landolfo E, Cutuli D, Petrosini L, Caltagirone C, Effects of Palmitoylethanolamide on Neurodegenerative Diseases: A Review from Rodents to Humans. Biomolecules (2022). doi: 10.3390/biom12050667.

[12]. Sagheddu C, Torres LH, Marcourakis T, Pistis M, Endocannabinoid-Like Lipid Neuromodulators in the Regulation of Dopamine Signaling: Relevance for Drug Addiction, Front. Synaptic Neurosci (2020). doi:10.3389/fnsyn.2020.588660.

[13]. Sagheddu C, Scherma M, Congiu M, Fadda P, Carta G, Banni S, Wood JAT, Makriyannis A, Malamas MS, Pistis M, Inhibition of N-acylethanolamine acid amidase reduces nicotine-induced dopamine activation and reward, Neuropharmacology (2019). doi:10.1016/j.neuropharm.2018.11.013.

[14]. Fotio Y, Palese F, Tipan PG, Ahmed F, Piomelli D, Inhbition of fatty acid amide hydrolase in the CNS prevents and reverses morphine tolerance in male and female mice. Br. J. Pharmacol (2020). doi: 10.1111/bph.15031

[15]. Readhead B, Haure-Mirande JV, Funk CC, Richards MA, Shannon P, Haroutunian V, Sano M, Liang WS, Beckmann ND, Price ND, Reiman EM, Schadt EE, Ehrlich ME, Gandy S, Dudley JT, Multiscale Analysis of Independent Alzheimer's Cohorts Finds Disruption of Molecular, Genetic, and Clinical Networks by Human Herpesvirus, Neuron (2018). doi:10.1016/j.neuron.2018.05.023.

[16]. Dauer W, Przedborski S, Parkinson's disease: Mechanisms and models, Neuron (2003). doi:10.1016/S0896-6273(03)00568-3.

[17]. William Langston J, Ballard P, Tetrud JW, Irwin I, Chronic parkinsonism in humans due to a product of meperidine-analog synthesis, Science (80–.) (1983). doi:10.1126/science.6823561.

[18]. Schober A, Classic toxin-induced animal models of Parkinson's disease: 6-OHDA and MPTP, Cell Tissue Res (2004). doi:10.1007/s00441-004-0938-y.

[19]. Kupsch A, Schmidt W, Gizatullina Z, Debska-Vielhaber G, Voges J, Striggow F, Panther P, Schwegler H, Heinze HJ, Vielhaber S, Gellerich FN, 6-Hydroxydopamine impairs mitochondrial function in the rat model of Parkinson's disease: Respirometric, histological, and behavioral analyses, J. Neural Transm (2014). doi:10.1007/s00702-014-1185-3.

[20]. Ueda N, Tsuboi K, Uyama T, Metabolism of endocannabinoids and related N-acylethanolamines: Canonical and alternative pathways, FEBS J (2013). doi:10.1111/febs.12152.

[21]. Ghidini A, Scalvini L, Palese F, Lodola A, Mor M, Piomelli D, Different roles for the acyl chain and the amine leaving group in the substrate selectivity of N-Acylethanolamine acid amidase, J. Enzyme Inhib. Med. Chem (2021). doi:10.1080/14756366.2021.1912035.

[22]. Park JH, Schuchman EH, Acid ceramidase and human disease, Biochim. Biophys. Acta - Biomembr (2006). doi:10.1016/j.bbamem.2006.08.019.

[23]. Do J, McKinney C, Sharma P, Sidransky E, Glucocerebrosidase and its relevance to Parkinson disease, Mol. Neurodegener (2019). doi:10.1186/s13024-019-0336-2.

[24]. Jackson-Lewis V, Przedborski S, Protocol for the MPTP mouse model of Parkinson's disease, Nat. Protoc (2007). doi:10.1038/nprot.2006.342.

[25]. Huang DW, Sherman BT, Lempicki RA, Systematic and integrative analysis of large gene lists using DAVID bioinformatics resources, Nat. Protoc (2009). doi:10.1038/nprot.2008.211.

[26]. Jiang H, Kang SU, Zhang S, Karuppagounder S, Xu J, Lee YK, Kang BG, Lee Y, Zhang J, Pletnikova O, Troncoso JC, Pirooznia S, Andrabi SA, Dawson VL, Dawson TM, Adult conditional knockout of PGC-1α leads to loss of dopamine neurons, ENeuro (2016). doi:10.1523/ENEURO.0183-16.2016.

[27]. Zheng B, Liao Z, Locascio JJ, Lesniak KA, Roderick SS, Watt ML, Eklund AC, Zhang-James Y, Kim PD, Hauser MA, Grünblatt E, Moran LB, Mandel SA, Riederer P, Miller RM, Federoff HJ, Wüllner U, Papapetropoulos S, Youdim MB, Cantuti-Castelvetri I, Young AB, Vance JM, Davis RL, Hedreen JC, Adler CH, Beach TG, Graeber MB, Middleton FA, Rochet JC, Scherzer CR, PGC-1α, a potential therapeutic target for early intervention in Parkinson's disease, Sci. Transl. Med (2010). doi:10.1126/scitranslmed.3001059.

[28]. Su X, Chu Y, Kordower JH, Li B, Cao H, Huang L, Nishida M, Song L, Wang D, Federoff HJ, PGC-1α promoter methylation in Parkinson's disease, PLoS One (2015). doi:10.1371/journal.pone.0134087.

[29]. Piccinin E, Sardanelli AM, Seibel P, Moschetta A, Cocco T, Villani G, PGC-1s in the spotlight with Parkinson's disease, Int. J. Mol. Sci (2021). doi:10.3390/ijms22073487.

[30]. Grünewald A, Kumar KR, Sue CM, New insights into the complex role of mitochondria in Parkinson's disease, Prog. Neurobiol (2019). doi:10.1016/j.pneurobio.2018.09.003.

[31]. Rocha EM, De Miranda B, Sanders LH, Alpha-synuclein: Pathology, mitochondrial dysfunction and neuroinflammation in Parkinson's disease, Neurobiol. Dis (2018). doi:10.1016/j.nbd.2017.04.004.

[32]. Stan AD, Ghose S, Gao XM, Roberts RC, Lewis-Amezcua K, Hatanpaa KJ, Tamminga CA, Human postmortem tissue: What quality markers matter?, Brain Res (2006). doi:10.1016/j.brainres.2006.09.025.

[33]. Jamwal S, Blackburn JK, Elsworth JD, PPARγ/PGC1α signaling as a potential therapeutic target for mitochondrial biogenesis in neurodegenerative disorders, Pharmacol. Ther (2021). doi:10.1016/j.pharmthera.2020.107705.

[34]. Gottschalk CG, Jana M, Roy A, Patel DR, Pahan K, Gemfibrozil protects dopaminergic neurons in a mouse model of Parkinson's disease via ppara-dependent astrocytic gdnf pathway, J. Neurosci (2021). doi:10.1523/JNEUROSCI.3018-19.2021.

[35]. Avagliano C, Russo R, De Caro C, Cristiano C, La Rana G, Piegari G, Paciello O, Citraro R, Russo E, De Sarro G, Meli R, Mattace Raso G, Calignano A, Palmitoylethanolamide protects mice against 6-OHDA-induced neurotoxicity and endoplasmic reticulum stress: In vivo and in vitro evidence, Pharmacol. Res (2016). doi:10.1016/j.phrs.2016.09.004.

[36]. Lama J, Buhidma Y, Fletcher EJR, Duty S, Animal models of Parkinson's disease: a guide to selecting the optimal model for your research, Neuronal Signal (2021). doi:10.1042/ns20210026.

[37]. Polinski NK, Volpicelli-Daley LA, Sortwell CE, Luk KC, Cremades N, Gottler LM, Froula J, Duffy MF, Lee VMY, Martinez TN, Dave KD, Best practices for generating and using alpha-synuclein pre-formed fibrils to model Parkinson's disease in rodents, J. Parkinsons. Dis (2018). doi:10.3233/JPD-171248.

[38]. Bloem BR, Okun MS, Klein C, Parkinson's disease, Lancet (2021). doi:10.1016/S0140-6736(21)00218-X.

[39]. Vijiaratnam N, Simuni T, Bandmann O, Morris HR, Foltynie T, Progress towards therapies for disease modification in Parkinson's disease, Lancet Neurol (2021). doi:10.1016/S1474-4422(21)00061-2.

[40]. Chahine LM, Beach TG, Brumm MC, Adler CH, Coffey CS, Mosovsky S, Caspell-Garcia C, Serrano GE, Munoz DG, White CL, Crary JF, Jennings D, Taylor P, Foroud T, Arnedo V, Kopil CM, Riley L, Dave KD, Mollenhauer B, In vivo distribution of α-synuclein in multiple tissues and biofluids in Parkinson disease, Neurology (2020). doi:10.1212/WNL.0000000000010404.

[41]. Hoss AG, Labadorf A, Beach TG, Latourelle JC, Myers RH, microRNA profiles in Parkinson's disease prefrontal cortex, Front. Aging Neurosci (2016). doi:10.3389/fnagi.2016.00036.

[42]. Beach TG, Adler CH, Sue LI, Serrano G, Shill HA, Walker DG, Lue L, Roher AE, Dugger BN, Maarouf C, Birdsill AC, Intorcia A, Saxon-Labelle M, Pullen J, Scroggins A, Filon J, Scott S, Hoffman B, Garcia A, Caviness JN, Hentz JG, Driver-Dunckley E, Jacobson SA, Davis KJ, Belden CM, Long KE, Malek-Ahmadi M, Powell JJ, Gale LD, Nicholson LR, Caselli RJ, Woodruff BK, Rapscak SZ, Ahern GL, Shi J, Burke AD, Reiman EM, Sabbagh MN, Arizona Study of Aging and Neurodegenerative Disorders and Brain and Body Donation Program, Neuropathology (2015). doi:10.1111/neup.12189.

[43]. Folstein MF, Folstein SE, McHugh PR, "Mini-mental state". A practical method for grading the cognitive state of patients for the clinician, J. Psychiatr. Res (1975). doi:10.1016/0022-3956(75)90026-6.

[44]. Emre M, Aarsland D, Brown R, Burn DJ, Duyckaerts C, Mizuno Y, Broe GA, Cummings J, Dickson DW, Gauthier S, Goldman J, Goetz C, Korczyn A, Lees A, Levy R, Litvan I, McKeith I, Olanow W, Poewe W, Quinn N, Sampaio C, Tolosa E, Dubois B, Clinical diagnostic criteria for dementia associated with Parkinson's disease, Mov. Disord (2007). doi:10.1002/mds.21507.

[45]. Bell CC, DSM-IV: Diagnostic and Statistical Manual of Mental Disorders, JAMA J. Am. Med. Assoc (1994). doi:10.1001/jama.1994.03520100096046.

[46]. McKhann GM, Knopman DS, Chertkow H, Hyman BT, Jack CR, Kawas CH, Klunk WE, Koroshetz WJ, Manly JJ, Mayeux R, Mohs RC, Morris JC, Rossor MN, Scheltens P, Carrillo MC, Thies B, Weintraub S, Phelps CH, The diagnosis of dementia due to Alzheimer's disease: Recommendations from the National Institute on Aging-Alzheimer's Association workgroups on diagnostic guidelines for Alzheimer's disease, Alzheimer's Dement (2011). doi:10.1016/j.jalz.2011.03.005.

[47]. Dellasega C, Morris D, The MMSE to assess the cognitive state of elders. Mini-Mental State Examination., J. Neurosci. Nurs (1993). doi:10.1097/01376517-199306000-00003.

[48]. Palese F, Pontis S, Realini N, Piomelli D, A protective role for N-acylphosphatidylethanolamine phospholipase D in 6-OHDA-induced neurodegeneration, Sci. Rep (2019). doi:10.1038/s41598-019-51799-1.

[49]. Zhu C, Solorzano C, Sahar S, Realini N, Fung E, Sassone-Corsi P, Piomelli D, Proinflammatory stimuli control NAPE-PLD expression in macrophages, Mol Pharmacol (2011). doi:mol.110.070201 [pii]\r10.1124/mol.110.070201 [doi].

[50]. Bonezzi FT, Sasso O, Pontis S, Realini N, Romeo E, Ponzano S, Nuzzi A, Fiasella A, Bertozzi F, Piomelli D, An important role for N-acylethanolamine acid amidase in the complete freund's adjuvant rat model of arthritis, J. Pharmacol. Exp. Ther (2016). doi:10.1124/jpet.115.230516.

[51]. Rauniyar N, Gao B, McClatchy DB, Yates JR, Comparison of protein expression ratios observed by sixplex and duplex TMT labeling method, J. Proteome Res (2013). doi:10.1021/pr3008896.

[52]. Shevchenko A, Tomas H, Havliš J, Olsen JV, Mann M, In-gel digestion for mass spectrometric characterization of proteins and proteomes, Nat. Protoc (2007). doi:10.1038/nprot.2006.468.
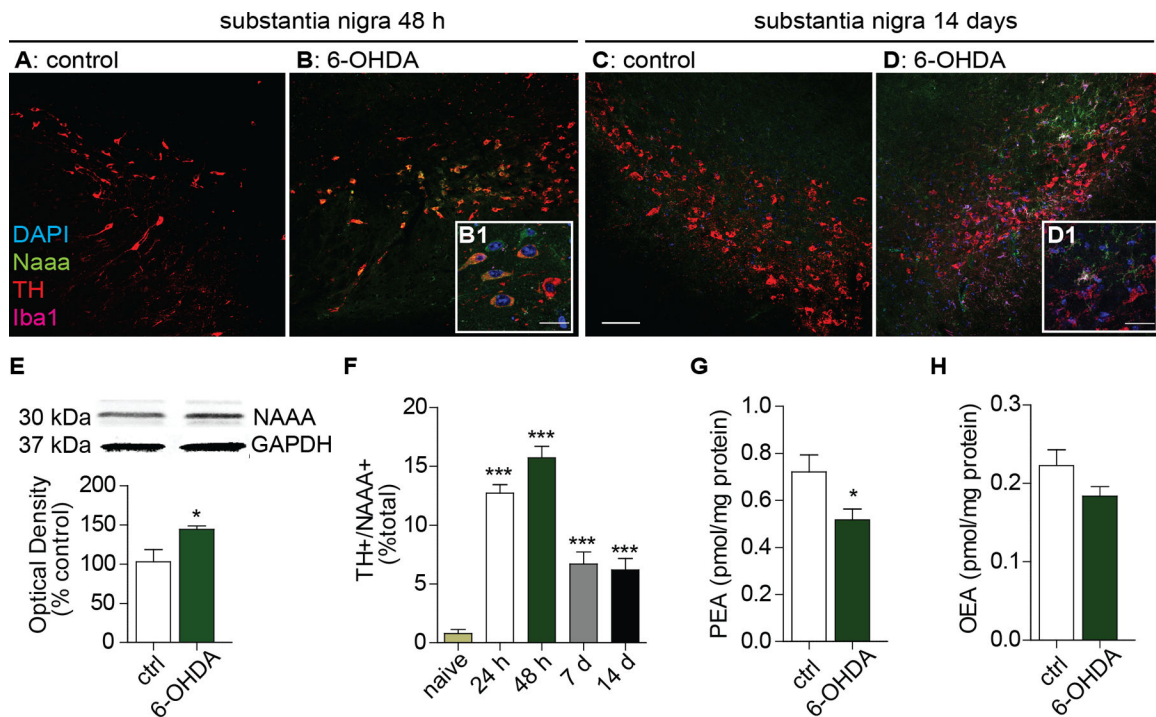
Figure 1. 6-OHDA and MPTP induce NAAA expression in human SH-SY5Y cells.
(**A**) Cell viability quantification in SH-SY5Y cells after incubation with vehicle (veh) or 6-OHDA (100 μM, 8h); ****P<0.0001 Student's *t* test (n=12). (**B, C**) Immunofluorescence images for TH (red) in SH-SY5Y cells after 8 h incubation with vehicle (**B**) or 6-OHDA (100 μM) (**C**). Cell nuclei were stained with 4',6-diamidino-2-phenylindole (DAPI, blue). Scale bar, 10 μm. (**D-E**) Immunofluorescence images for NAAA (green) in SH-SY5Y cells after incubation with vehicle (**D**) or 6-OHDA (**E**); cell nuclei were stained with DAPI. (**F**) RT-PCR quantification of *Naaa* mRNA in SH-SY5Y cells after incubation with vehicle (veh) or 6-OHDA (2–8h); ***P<0.001, one-way ANOVA followed by Bonferroni post hoc test (n=3). (**G**) PEA levels in SH-SY5Y cells after incubation with 6-OHDA (2–8h) or vehicle; *P<0.05, one-way ANOVA and Bonferroni (n=6). (**H-I**) NAAA activity (**H**) and NAAA protein quantification (**I**) in exosomes released by SH-SY5Y cells; **P<0.01, *P<0.05 Student's *t* test (n=3). (**J**) Cell viability quantification in SH-SY5Y cells after incubation with vehicle (veh) or MPP⁺ (2 μM, 24h); ****P<0.0001 Student's *t* test (n=12). (**K-L**) Immunofluorescence images of NAAA (green) in SH-SY5Y cells after 24 h incubation with vehicle (**K**) or MPP⁺ (**L**). Scale bar, 10 μm; cell nuclei were stained with DAPI. (**M**) RT-PCR quantification of *Naaa* mRNA in SH-SY5Y cells after incubation with 2 mM MPP⁺ (4–24h) or vehicle; ***P<0.001, **P<0.01 one-way ANOVA and Bonferroni (n=3). (**N**) PEA levels in SH-SY5Y cells after incubation with MPP⁺ (8–48h) or vehicle (n=6).
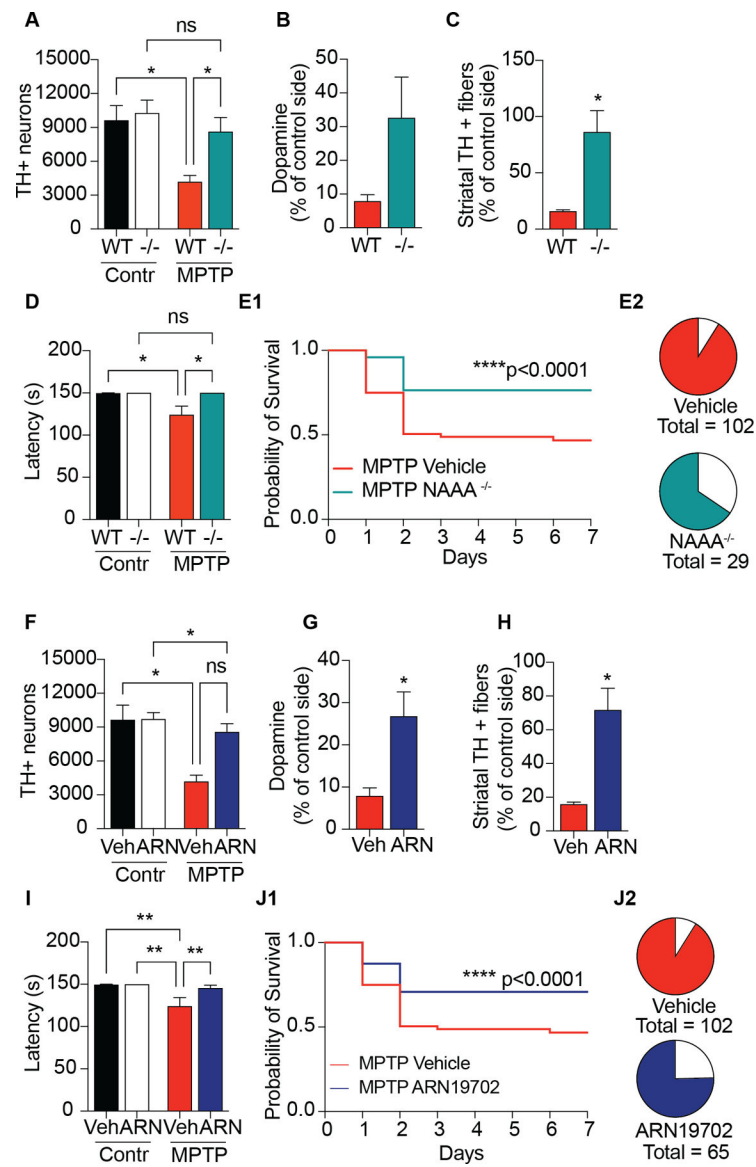
Figure 2. 6-OHDA induces rapid and persistent NAAA expression in nigrostriatal dopamine neurons.

(**A-D**) Merged immunofluorescence images for NAAA (green), TH (red) and ionized calcium-binding adaptor molecule 1 (Iba-1, magenta) in tissue sections of SN pars compacta: (**A, C**) control and (**B, D**) lesioned (ipsilateral and contralateral, respectively, to the 6-OHDA injection site); cell nuclei were stained with DAPI (blue). Images were collected 48 h (**A, B**) or 14 days (**C, D**) after 6-OHDA injection. NAAA[+]/TH[+] co-localization is shown in yellow, NAAA[+]/Iba-1^{+} co-localization is shown in white. Scale bar, 50 μm. (**B1, D1**) High-magnification images of NAAA^{+} cells that co-express (**B1**) TH or (**D1**) Iba-1. Scale bar, 10 μm. (**E**) Western blot quantification of NAAA in midbrain fragments containing the SN 48 h after 6-OHDA administration: top, representative blot; bottom, densitometric quantification. Glyceraldehyde 3-phosphate dehydrogenase (GAPDH) was used for normalization. *P<0.05, two-tailed Student's *t* test (n=5). (**F**) Number of neurons co-expressing TH and NAAA, shown as percent of total TH^{+} neurons in SN pars
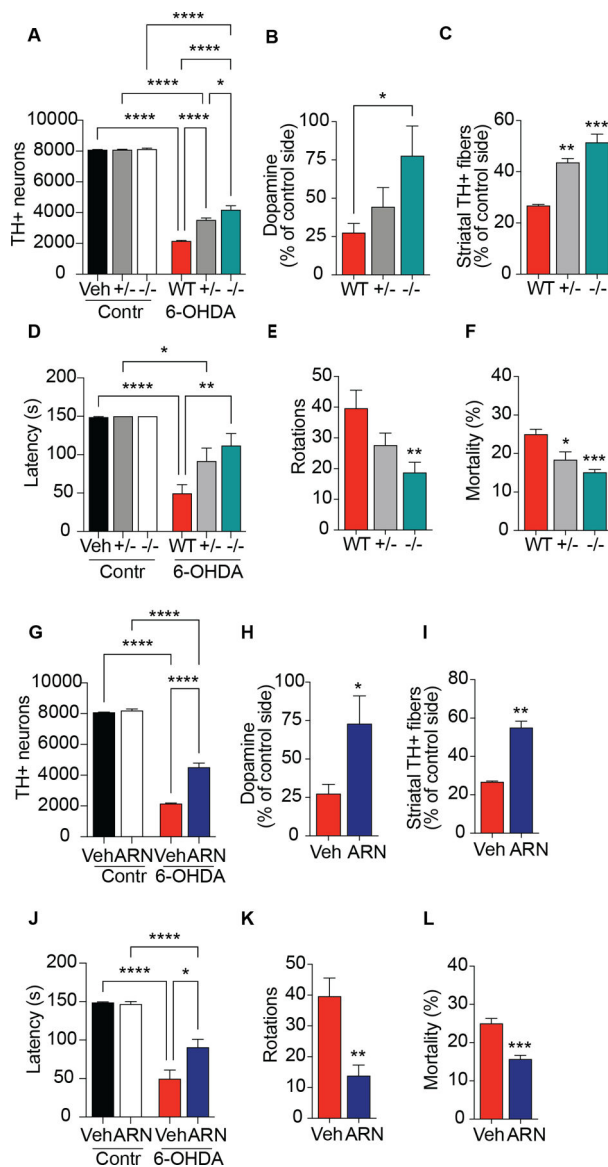
compacta. ***P<0.001, one-way ANOVA with Bonferroni post hoc test (n=4). (**G, H**) (**G**) PEA and (**H**) OEA quantification midbrain fragments containing the SN 48 h after 6-OHDA injection. *P<0.05, two-tailed Student's *t* test (n=5).

Figure 3. 6-OHDA causes delayed NAAA expression in striatal microglia.
(**A**) Transcription of pro-inflammatory cytokines (tumor necrosis factor-a, TNF-α; interleukin 6, IL-6; interleukin-1β, IL-1β; and interferon-γ, IFN-γ) in control (open bars) and lesioned (red bars) striata 14 days after 6-OHDA injection. ***P<0.001, **P<0.01, *P<0.05, two-tailed Student's *t* test (n=5). (**B-D**) Immunofluorescence images of sections from (**B**) intact and (**C, D**) lesioned striatum: cell nuclei are stained with DAPI (blue); NAAA is shown in green, Iba-1 in magenta; merged NAAA/Iba-1 signals are shown in yellow. Scale bar, 10 μm. (**E, F**) Immunofluorescence images of sections from (**E**) intact and (**F**) lesioned striatum. Scale bar, 50 μm. (**E1, F1**) High-magnification images of Iba-1^{+} microglial cells in sections from intact (**E1**) and lesioned (**F1**) striata. Scale bar, 10 μm.
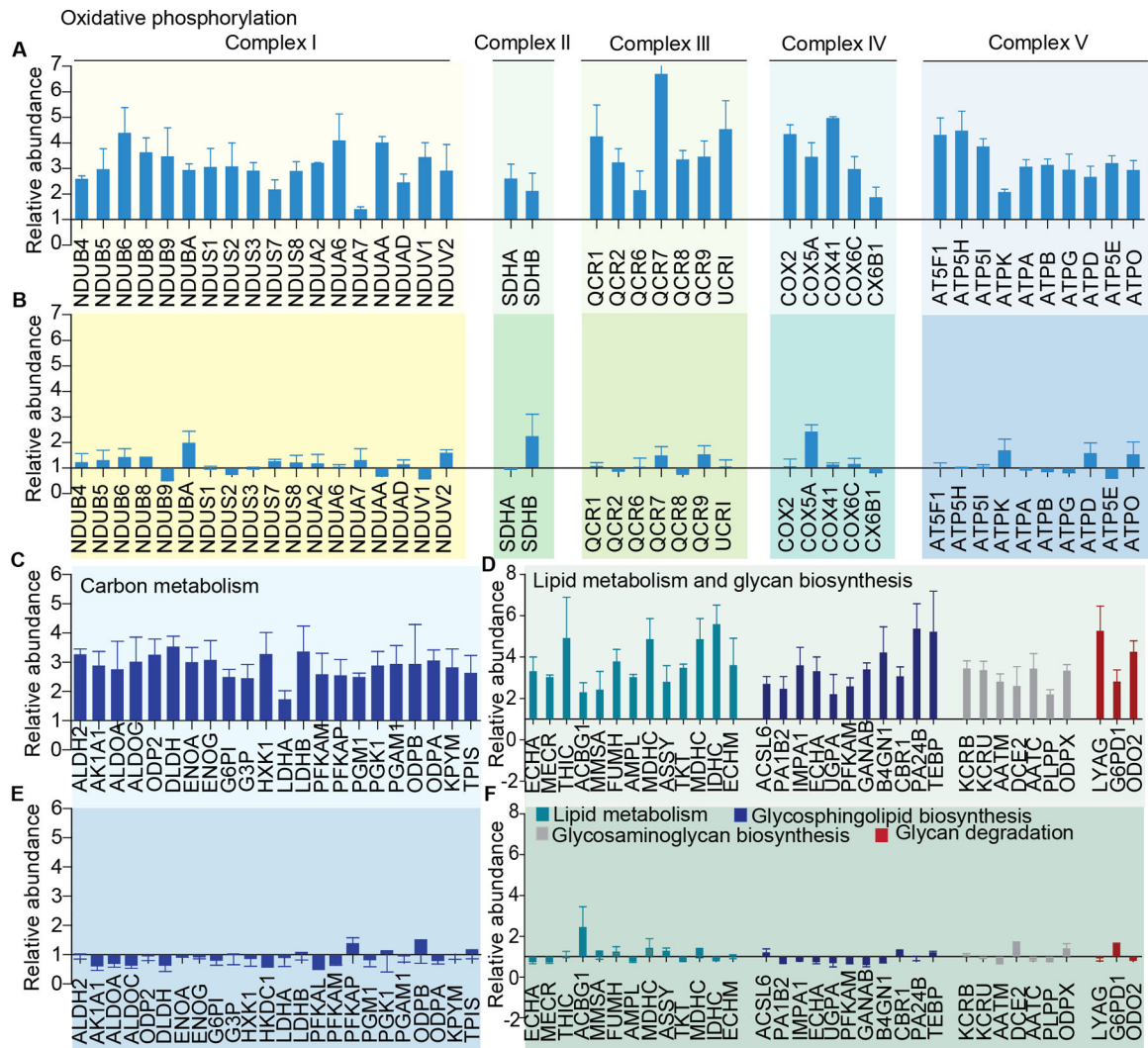
Figure 4. Genetic NAAA deletion and pharmacological NAAA inhibition protect mice from 6-OHDA-induced neurotoxicity.

(**A, G**) Number of TH$^+$ neurons in SN pars compacta; ****P<0.0001, *P<0.01 two-way ANOVA followed by Bonferroni post hoc test (n=4). (**B, H**) Striatal dopamine content; *P<0.05, compared to intact side, one-way ANOVA followed by Tuckey post hoc test (**B**) or Student's t test (**H**) (n=4). (**C, I**) Density of striatal TH$^+$ fibers, expressed as percent of intact side. ***P<0.001, **P<0.01, one-way ANOVA and Tuckey (**C**) or Student's t test (**I**) (n=6). (**D, J**) Performance in the rotarod test (latency to fall, s); naïve mice (no 6-OHDA injection) are shown for comparison. ****P<0.0001, **P<0.01, *P<0.05, two-way ANOVA and Bonferroni (n=8). (**E, K**) Apomorphine-induced rotations. **P<0.01 compared to WT vehicle-treated mice, one-way ANOVA and Tuckey (**E**) or Student's t test (**K**) (n=8). (**F, L**) Mortality rate; ***P<0.001, *P<0.05, compared to wild-type (WT) mice, one-way ANOVA and Tuckey (**F**) or Student's t test (**L**) (n=16). Measurements were performed 21 days after 6-OHDA injection.
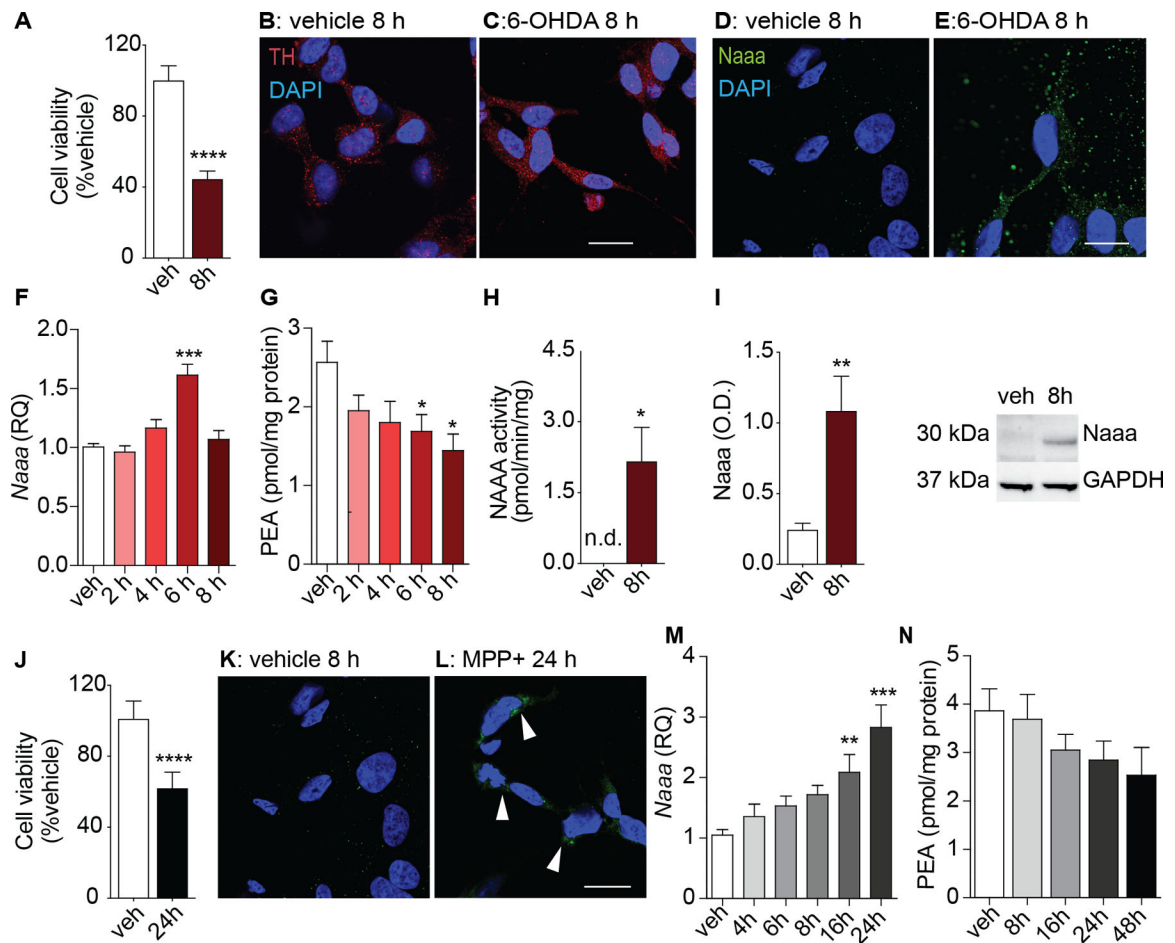
Figure 5. Genetic NAAA deletion and pharmacological NAAA inhibition protect mice from MPTP-induced neurotoxicity.

(**A, F**) Number of TH$^+$ neurons in SN pars compacta; *P<0.05 two-way ANOVA followed by Bonferroni post hoc test (n=3–5). (**B, G**) Striatal dopamine content (n=3–4). (**C, H**) Density of striatal TH$^+$ fibers, expressed as percent of controls; *P<0.05, Student's *t* test (n=3–4). (**D, I**) Performance in the rotarod test (latency to fall, s); naïve mice (no MPTP injection) are shown for comparison; *P<0.05, two-way ANOVA and Bonferroni (n=3–10). (**E1, J1**) Survival rate. ****P<0.001, Log-rank test (n=29–102). (**E2, J2**) Total number of animals survived after MPTP administration. Measurements were performed 7 days after MPTP injection.

Figure 6. *Naaa*^{−/−} mice differentially regulate bioenergetic pathways in response to 6-OHDA.
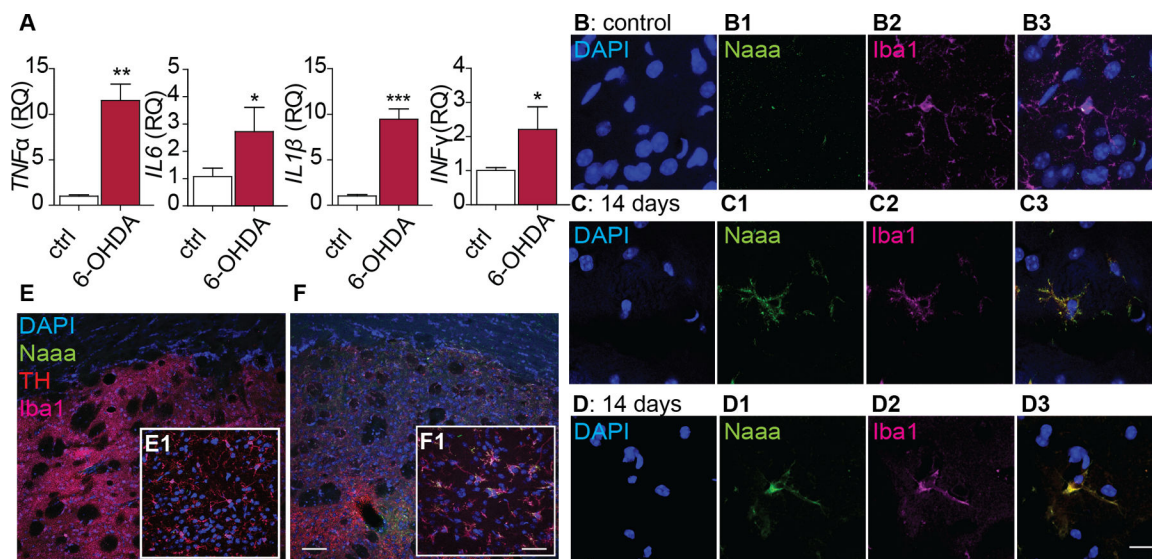
Figure 6. $Naaa^{-/-}$ mice differentially regulate bioenergetic pathways in response to 6-OHDA.
(**A, C, E**) Comparative proteomics analysis of lesioned SN ($Naaa^{-/-}$ versus wild-type, WT) 48 h after 6-OHDA administration: (**A**) oxidative phosphorylation; (**C**) carbon metabolism; and (**E**) lipid and glycan metabolism. (**B, D, F**) Comparative proteomics analysis of intact SN ($Naaa^{-/-}$ versus WT): (**B**) oxidative phosphorylation; (**D**) carbon metabolism; and (**F**) lipid and glycan metabolism.
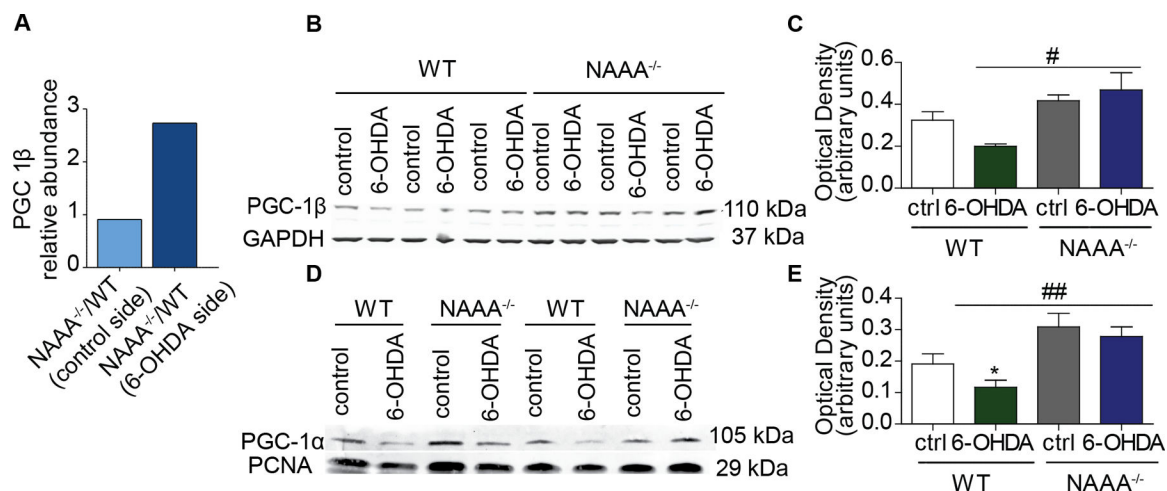
Figure 7. 6-OHDA suppresses expression of bioenergetic pathways in a NAAA-dependent manner.

(**A**) Relative abundance (*Naaa*$^{-/-}$ versus WT) of PGC-1β in control (light blue) and lesioned (dark blue) SN. (**B-E**) Representative western blots and densitometric quantification of (**C**) PGC-1β in nigral homogenates, and (**E**) PGC-1α in nuclear fractions of SN tissue from WT and *Naaa*$^{-/-}$ mice 48 h after 6-OHDA administration. GAPDH and proliferating cell nuclear antigen (PCNA) were used for normalization. *P<0.05 compared to wild-type (WT) contralateral side; #P<0.05 and ## P<0.01, compared to lesioned side of WT/veh mice, two-way ANOVA followed by Bonferroni post hoc test (n=4).
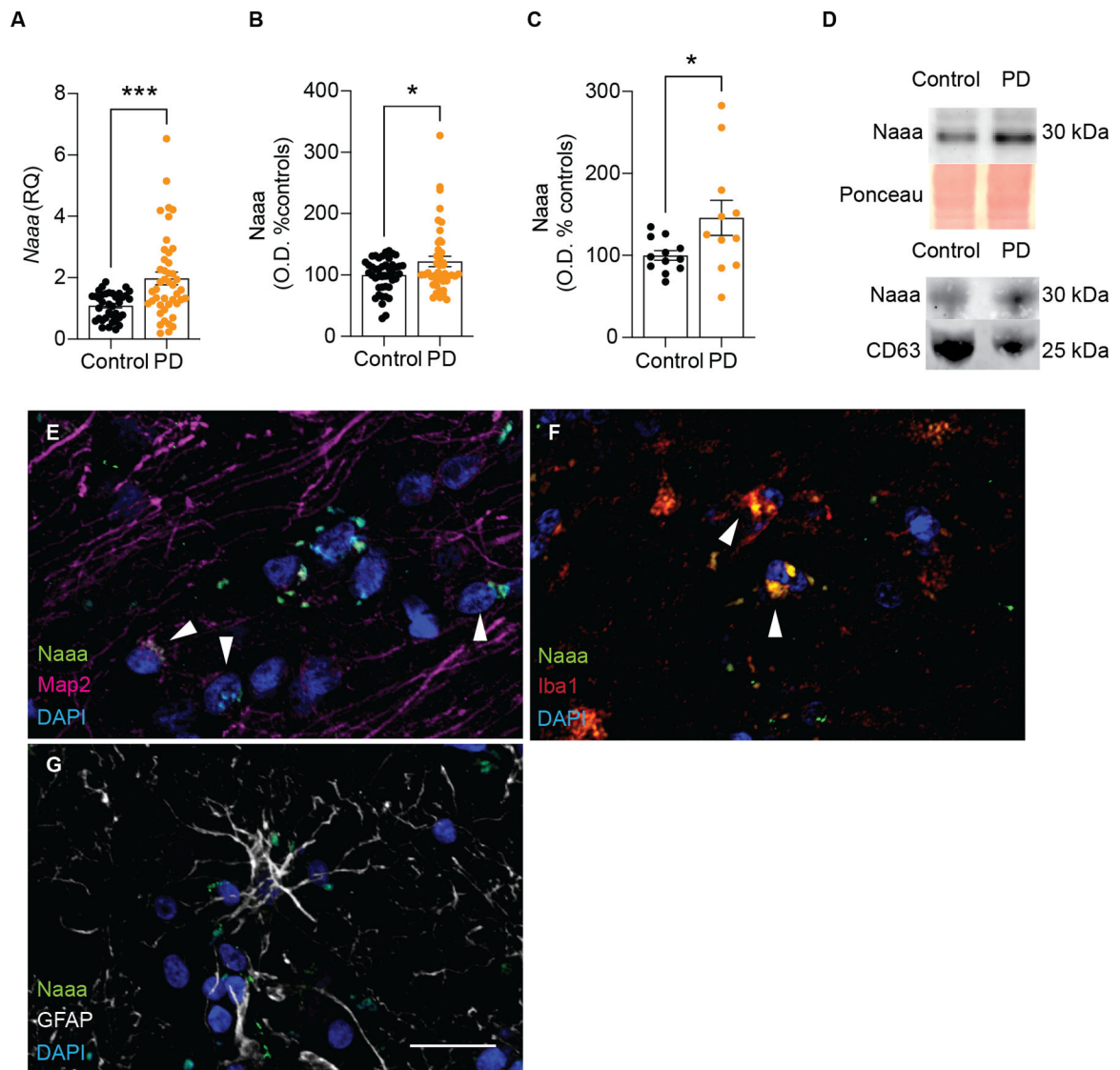
Figure 8: NAAA levels in persons with Parkinson's disease.
(**A, B**) RT-PCR quantification of *Naaa* mRNA (**A**) and densitometric analyses of NAAA protein (**B**) in postmortem cortex specimens from persons with PD (n=43) and age- and sex-matched controls (n=46). (**C**) Western blot analysis of NAAA protein in circulating exosomes obtained from plasma of persons with PD (n=11) and age- and sex-matched controls (n=12). (**D**) Representative blots: Ponceau staining (full label) was used for normalization of cortex samples, CD63 for exosomes samples. ***P<0.001, *P<0.05, Student's *t* test. (**E-G**) Representative confocal images of immunostaining in cortex from a patient with PD. Merged immunofluorescence images for NAAA (green, **E-G**), Map2 (magenta, **E**), Iba1 (red, **F**), GFAP (white, **G**). Cell nuclei were stained with DAPI (blue). Scale bar, 20 μm.